Ion-scattering study and Monte Carlo simulations of surface segregation in Pd-Pt nanoclusters obtained by laser vaporization of bulk alloys

J. L. Rousset,* A. J. Renouprez, and A. M. Cadrot
Institut de Recherches sur la Catalyse, CNRS, 2 avenue A. Einstein, F69626, Villeurbanne CEDEX, France
(Received 14 August 1997; revised manuscript received 23 February 1998)

Bimetallic Pd-Pt clusters deposited on amorphous carbon have been produced by laser vaporization of various bulk alloys. Energy dispersive x-ray analysis and transmission electron microscopy show that they have a perfectly well-defined stoichiometry and a narrow range of size. They constitute ideal systems to investigate segregation processes in finite solids. It is shown that low-energy ion scattering allows the determination of surface concentration, which has been found to be different from the overall one. Monte Carlo simulations coupled with a recently developed energetical model, based on a tight-binding scheme that includes bond strength modifications at surfaces, account well for the experimental finding and give information on the surface distribution of the segregating Pd atoms. [S0163-1829(98)06628-4]

I. INTRODUCTION

Bimetallic clusters constitute an exciting field of research due to the interest they generate both from the theoretical and applied points of view. It is generally recognized that a compulsory passage in the development of a new catalyst is the control of its properties, and, in particular, of its surface composition and local order at the atomic scale that directs its electronic and hence chemical properties. The association of two metals can lead to catalysts exhibiting considerably improved activity and selectivity compared to those of each component.[1–2] This is the case of the bimetallic Pd-Pt catalyst used in industry for hydrogenation of aromatics in diesel oil.[3] Basically, the techniques available to measure the surface composition of a dispersed solid can be classified as follows: chemisorption techniques such as volumetry or temperature programmed desorption, optical techniques (IR, UV, Raman, etc.), electron or Auger spectroscopies, and ion beam techniques [low-energy ion scattering (LEIS), and secondary ion/neutral mass spectroscopy (SIMS, SNMS)]. All these techniques have their specific characteristics and have their place in the task of the complete characterization of a dispersed material. If, however, we focus our attention on the capability of providing data about the *topmost* atomic layer only, i.e., where catalytic reactions occur, we see that only two methods can do that: ''chemical'' and ion beam techniques. Chemical titration of the active sites has several drawbacks such as a low elemental discrimination, a frequently unknown adsorption stoichiometry, and a possible modification of the surface composition. Regarding ion beam techniques, LEIS allows us to measure selectively the composition of the topmost atomic layer of a solid[4–7] (a fact that was demonstrated 20 years ago) and, to our knowledge, is the only one able to provide such information. This feature is of obvious importance in catalysis especially in view of the possible control of the catalyst surface composition and structure at the nanometer scale. Yet, LEIS in catalytic studies is not routinely used for material characterization. On the contrary, numerous studies reported in the literature[8] have shown that the quantification of LEIS data is relatively easy for simple flat systems (e.g., binary single crystals or polycrystalline alloys) provided that the mass of the different elements differ by more than about 5%. However, one has to be careful in performing ion-scattering experiments on small clusters because damage by sputtering does occur and the sputter yield of clusters may be significantly larger than that of the bulk.[9] The knowledge of the surface structure should, in principle, facilitate the understanding of the reactivity of metal alloy clusters. Most bimetallic clusters are prepared in a chemical way, i.e., by coimpregnation or coexchange techniques but large distributions of composition are generally observed.[10,11] It is thus difficult to study the relation between surface and bulk composition. Laser vaporization is a method of choice for generating ligand-free metal clusters because it can be used to evaporate even the most refractory metals. In the case of bimetallic systems, the advantage of this technique becomes essential since, as will be shown in the following, the composition of each produced particle is identical to that of the vaporized rod. The aim of this work is to show that it is possible to produce clusters with well-defined size and stoichiometry and to study experimentally their overall surface composition.

Concerning cluster study, even if experimental data are scarce, theoretical results are available which often deal with cluster structure,[12–14] ordering and segregation processes.[15,16] The equilibrium cluster structure can be computed using Monte Carlo simulations with the energetics described by a modified tight-binding (MTB) scheme.[17–19] The advantage of the Monte Carlo (MC) approach is that it can provide a view of the microscopic arrangements and the location of the different atoms which, at present, cannot be measured experimentally for small clusters. Thus, the Monte Carlo technique can be assumed to be reliable if the overall surface concentration is found to be in good quantitative agreement with the experimental data.

II. CLUSTER PRODUCTION AND CHARACTERIZATION

A. Experimental setup and free cluster properties

The laser vaporization cluster source has been extensively described elsewhere[18] and has been designed for the most

part according to the source of Milani and de Heer.[20] Briefly, a Nd:YAG laser is focused onto a metallic rod, which is driven in a slow screw motion. Synchronized with the laser pulse, a short intense helium burst delivered by a fast pulsed valve cools the laser-induced plasma. A further cooling and cluster condensation occur at the output nozzle of the source because the instantaneous pressure in the source chamber rises high enough to produce an efficient isentropic supersonic expansion at the exit of this chamber. Typical deposition rates around 0.1 nm/min are obtained with neutral clusters of various materials. The deposition is carried out in a UHV chamber coupled to the source. For the experiments described in the present work we have used two bimetallic rods obtained by melting palladium (99.99% purity) and platinum (99.95% purity) leading to atomic compositions of $Pd_{17}Pt_{83}$ and $Pd_{65}Pt_{35}$. Free clusters are analyzed by a perpendicular time-of-flight mass spectrometer. The properties of mixed Pd-Pt clusters in the gas phase have already been analyzed by mass spectroscopy and photofragmentation techniques for the $Pd_{65}Pt_{35}$ and $Pd_{17}Pt_{83}$ stoichiometries.[18] The main results were that, even for small sizes (number of atoms <10), the clusters are already bimetallic systems. The deposition rate of neutral aggregates is monitored using a quartz microbalance. The clusters have been deposited onto a thin amorphous carbon film evaporated on a copper grid in order to perform transmission-electron-microscopy experiments. The residual pressure in the deposition chamber was about 10^{-10} mbar and the equivalent deposited thickness is 0.2 nm. Once the samples are produced, they are either exposed to air and characterized by energy dispersive x-ray analysis (EDX) in a transmission-electron microscope (TEM) (JEOL 2010 or JEOL 2010*F*) operating at 200 kV or transferred in an UHV suitcase equipped with an ionic pump (5×10^{-9} mbar) into an ESCALAB 200*R* machine (from Fisons Instruments) where LEIS experiments are carried out (base pressure 1×10^{-10} Torr). For EDX spectroscopy, the spatial resolution was about 1 nm. The detector cutoff allows the detection of elements with atomic numbers $Z\geqslant4$.

B. Size and composition distributions measured by TEM and EDX

There are only scarce results on the nucleation of deposited clusters.[21] The cluster diffusion on the surface of amorphous carbon is certainly weak because the large number of defects on this surface act as traps for the particles, as demonstrated by the very similar particle diameters observed for different deposited thicknesses. Consequently, for low deposits the supported particles are well separated and homogeneously distributed on the substrate. This is shown in Fig. 1, which represents TEM images obtained with a 0.2-nm equivalent thickness deposit on *a-C* for both alloys. The size histograms, corresponding to 783 and 340 analyzed particles, respectively, for the $Pd_{17}Pt_{83}$ and $Pd_{65}Pt_{35}$ alloys, are shown in Fig. 2. The mean cluster sizes (standard deviations) are about 2.4 nm (0.54 nm) for $Pd_{17}Pt_{83}$ and 2.5 nm (0.6 nm) for $Pd_{65}Pt_{35}$. The observed sizes and dispersions are similar for both alloys and roughly the same as those obtained by vapodeposition of atoms.[22] However, in contrast to the vapodeposition technique, the mean cluster size is, in our case, independent of the equivalent deposited thickness.

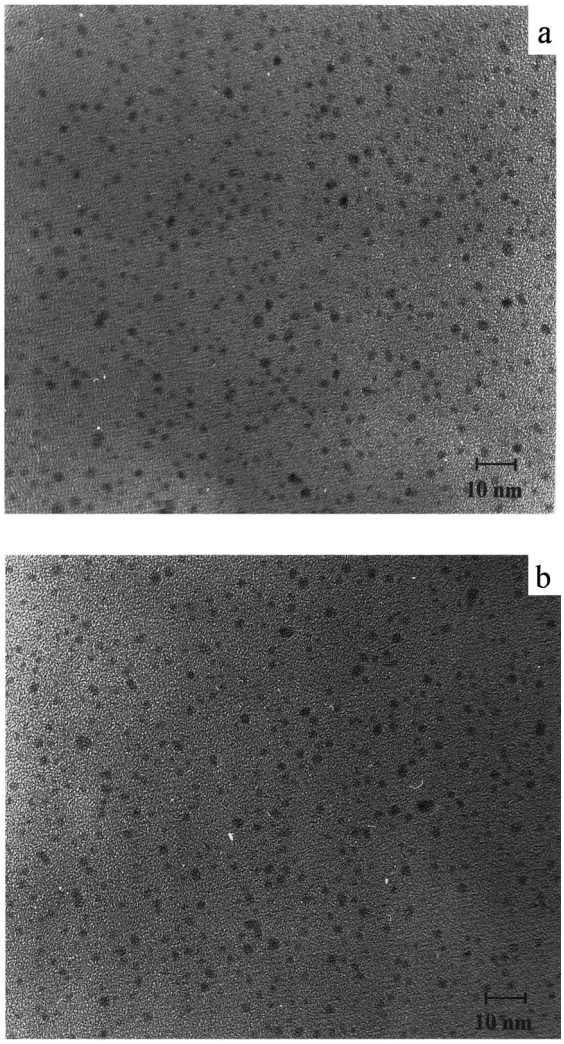

FIG. 1. TEM photographs of a 0.2-nm equivalent thickness deposit on amorphous carbon. (a) and (b) correspond, respectively, to $Pd_{17}Pt_{83}$ and $Pd_{65}Pt_{35}$ alloys.

Energy dispersive x-ray analysis is very convenient for studying the composition of bimetallic catalysts. It allows us to study individual particles by reducing the probe area down to 1 nm^2 and the composition homogeneity can be checked. Figure 3 shows composition histograms corresponding to the

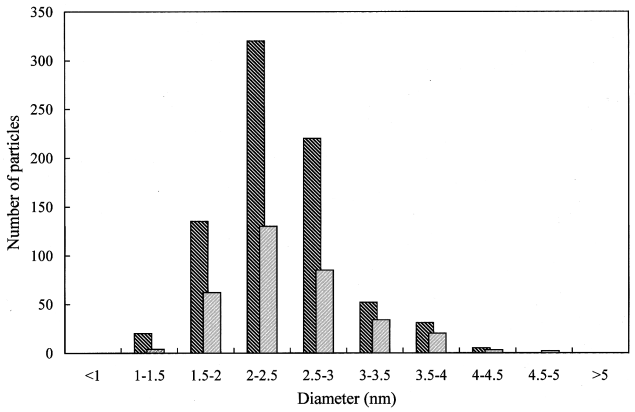

FIG. 2. Size distribution histograms of $Pd_{17}Pt_{83}$ (black line) and $Pd_{65}Pt_{35}$ (gray line) deposits.

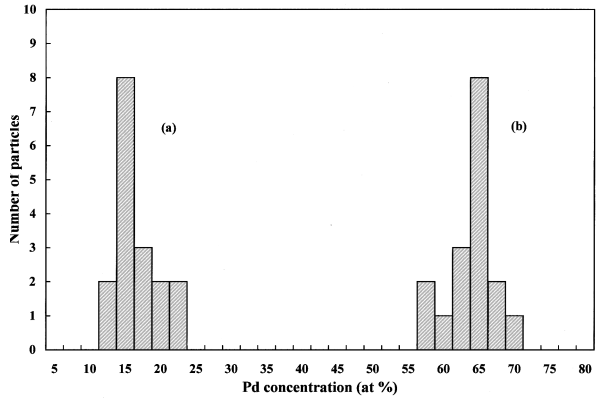

FIG. 3. Histogram of the palladium concentration of a collection of Pd-Pt supported clusters obtained from (a) $Pd_{17}Pt_{83}$ and (b) $Pd_{65}Pt_{35}$ rods.

analysis of a collection of isolated particles for the $Pd_{65}Pt_{35}$ and $Pd_{17}Pt_{83}$ alloys. One has to note that for the alloy with the lower Pd content, the sensitivity of the JEOL 2010 is not sufficient to extract the Pd signal from the background if only one particle is probed. So, the experiments on this alloy have been carried out in a microscope equipped with a field emission gun and that allows high-performance EDX measurements (JEOL 2010*F*). A quantitative analysis of the spectra gives then a composition nearly equal to that of the initial rod for both alloys, as shown in Fig. 3. The homogeneity of composition of the particles ensures that LEIS will give reliable results with respect to surface versus bulk composition of the particles.

III. SURFACE COMPOSITION MEASURED BY LEIS

The surface composition of alloys, and especially the composition of the topmost surface layer, is generally different from the bulk one due to segregation processes.[8] The low-energy ion scattering technique is a surface-sensitive technique that selectively probes the outermost atomic layer and is therefore well adapted to the study of surface segregation as has been shown for various flat surfaces of bimetallic alloys.[4,6,7,23,24] However, when performing ion-scattering experiments on particles, damage can occur more easily than for massive systems because the sputter yield of clusters has been shown to be larger than that of the bulk.[9] A beam of monoenergetic (E_0) $^4He^+$ ions of mass M_1 is focused on the surface of interest. Some of these ions are backscattered from the surface through an angle θ and their energy distribution is analyzed. The intensity of the LEIS signal depends on several factors and, in particular, on the probability of neutralization of the ions. Whereas the survival probability of the ionized state is of the order of 1–2 % for collisions involving the first atomic layer, it is effectively zero for those ions that penetrate below the first layer. This phenomenon is what makes LEIS so surface sensitive. The position of the elastic ion peak is given by

$$E/E_0=(M_1/M_1+M_2)^2[\cos\ \theta+\{(M_2/M_1)^2-\sin^2\theta\}^{1/2}]^2, \tag{1}$$

where M_2 is the mass of the surface atom involved in the collision. One has to mention that this equation holds only for binary collisions.

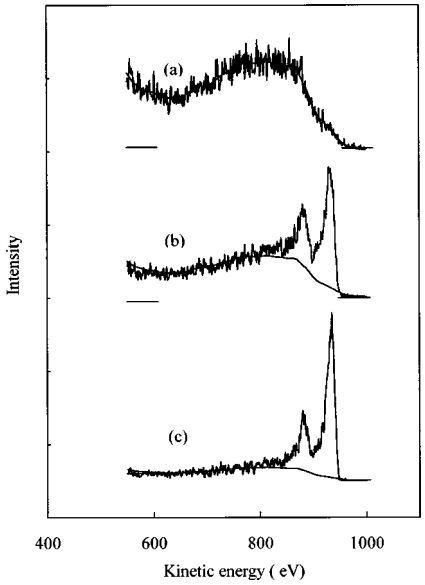

FIG. 4. (a) Background shape due to low mass contaminants as obtained during the first acquisition on the $Pd_{17}Pt_{83}$ sample. The fitting curve is also represented. (b) and (c) are LEIS spectra before background removal.

LEIS analysis was performed with 1-keV $^4He^+$ ions at room temperature at a scattering angle θ of 142°. The primary beam intensity was 10 nA, focused on an impact spot of about 0.5 mm diameter. Reference samples used for the intensity calibration of the LEIS spectra were pure Pd and Pt single crystals of, respectively, (100) and (111) orientation. From the LEIS peak areas of the pure samples, the relative sensitivity factor S_{Pd}/S_{pt} was found to be 1.2. During the first acquisition period, represented in Fig. 4(a), no signals corresponding to Pd or Pt are observed and this corresponds to the background. After vertical scaling and smoothing, it is subtracted from the other spectra as shown for example in Figs. 4(b) and 4(c). Two peaks are clearly distinguishable at about 865 and 920 eV, corresponding to ions backscattered, respectively, by Pd and Pt surface atoms. These values are slightly smaller than those predicted by Eq. (1), because inelastic events cause peak shifts to lower energy and asymmetric peaks. Coupled with successive scatterings, they give rise to low-energy tails in the LEIS spectra. Figures 5 and 6 show typical LEIS spectra corresponding, respectively, to $Pd_{17}Pt_{83}$ and $Pd_{65}Pt_{35}$ deposits and their transformation during the ion bombardment. Each spectrum is the sum of spectra acquired after the same sputtering time on four different areas of the same sample. The differences between the individual spectra were negligible. For each spectrum, the background has been removed and fitting curves are represented. For both cases, after a few minutes of sputtering, a third signal centered at approximately 800 eV appears corresponding to copper. This signal is produced by Cu grid areas where carbon should have been locally removed by the ion beam. The small overlaps between the Pd, Pt, and Cu contributions allow an easy decomposition of each contribution. With increasing measurement time, a decrease of the Pd contribution with respect to the Pt one is observed and one can note also an improvement of the signal-to-noise ratio. This can be easily understood. LEIS is very sensitive to surface contamination, which neutralizes ions and/or causes energy

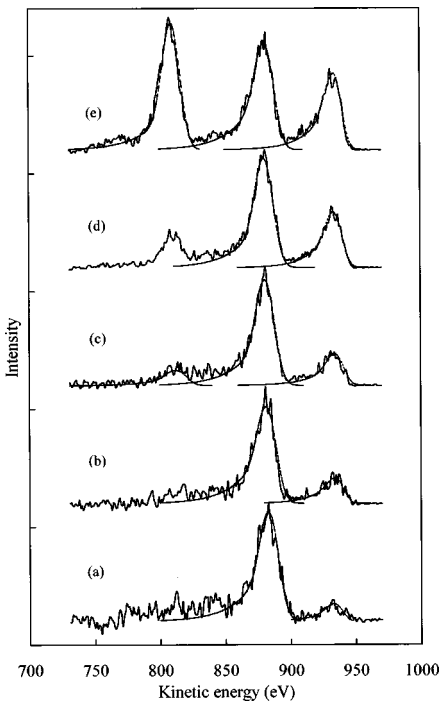

FIG. 5. Evolution of the LEIS signal during the $^4He^+$ 1-keV ion bombardment of the $Pd_{65}Pt_{35}$ sample after (a) 75, (b) 210, (c) 660, (d) 1335, and (e) 2235 sec sputtering time. The Pd and Pt signals are located at about 870 and 920 eV.

loss: so the sample has to be cleaned to observe a signal. During the bombardment, the total ion yield increases because of the desorption of low mass contaminants (O, H, and C). Even at such low energies, and low projectile mass, prolonged bombardment causes sputtering of surface atoms, not necessarily with the same efficiency for the Pd and Pt (preferential sputtering). So the continuous decrease of the Pd signal as compared to that of Pt should be interpreted as the combined effect of sputtering of the Pd-enriched surface and preferential sputtering of Pd. To quantify the surface concentration, peak areas (and not maximal intensities) should be used because they appropriately account for the isotopic mass distribution.

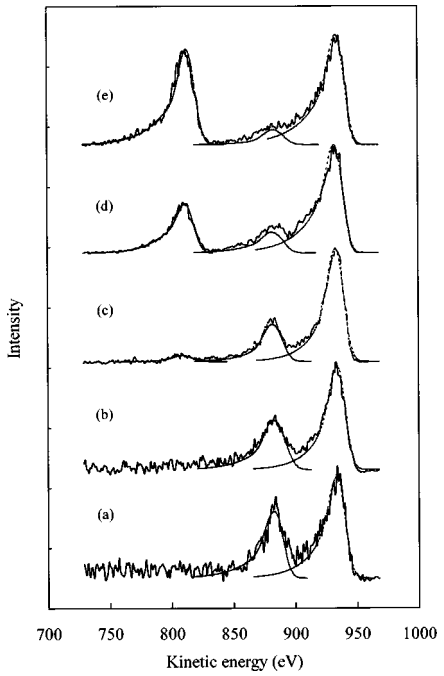

FIG. 6. Evolution of the LEIS spectrum during $^4He^+$ 1-keV ion bombardment of the $Pd_{17}Pt_{83}$ sample after (a) 75, (b) 165, (c) 210, (d) 660, and (e) 1785 sec sputtering time.

For the correct interpretation of the spectra, a curve synthesis procedure was applied. To fit the shape of the spectra, a sum of Gaussian and exponentially modified Gaussian functions was used. The exponential tails account for inelastic events. The broadening effect by isotopes is included. Fitting parameters are amplitudes, positions, widths of the Gaussians and areas, positions, widths, and distortions of the inelastic tails. However, it might be that the contamination layer reduces the sensitivity for Pd and Pt not in the same way. To make sure that the ratio between the Pd and Pt intensities, equated to the Pd/Pt surface concentration ratio, is reliable, an additional experiment was performed. A thin slice (about 1 mm) of the $Pd_{65}Pt_{35}$ rod has been cut and then mechanically polished down to 1 μm. Then the peak intensities of the 1-keV helium ions scattered by Pd and Pt as a function of the sputtering time have been measured. After about two hours of He ions (1 keV) bombardment the intensities reached constant values and we found, after quantitative analysis, a Pd surface equilibrium concentration (under sputtering) of 49%. The sample was then exposed to the same residual atmosphere as seen by the clusters during a few hours so that the surface is contaminated again. Then a second series of measurements of Pd and Pt intensities, as a function of sputtering time, was performed. The absolute intensities with the deduced Pd surface concentrations are shown in Fig. 7. Due to contaminants desorption, the absolute Pd and Pt intensities strongly increase with sputtering time whereas the corresponding Pd concentration remains nearly constant and equal to the value found before exposure to contamination. This clearly evidences that contaminants do not affect significantly the determined Pd surface concentration in the case of Pd-Pt alloys and that both metals are equally affected by the contamination.

Going over to the clusters study, the results of the fitting procedure are presented in Fig. 8. Clearly the two samples have a large Pd concentration (after applying a relative sensitivity factor of 1.2) in the first surface layer compared to the bulk one. The surfaces of the $Pd_{17}Pt_{83}$ and the $Pd_{65}Pt_{35}$ samples are enriched in Pd, respectively, up to about 38% and 87% as deduced from the spectra shown in Figs. 5(a) and 6(a).

This agrees, at least qualitatively, with the results of van den Oetelaar,[25] who found Pd segregation in both bulk bimetallic Pd-Pt alloys and industrial alumina supported Pd-Pt catalysts prepared at the Shell Research Technology Centre in Amsterdam. Indeed, for a $Pd_{73}Pt_{27}$/C catalyst (whose mean particle diameter is close to 5 nm), a Pd surface fraction of about 0.95 has been measured after annealing at 673 K. Due to the ion bombardment (which induces sputtering effects and ion beam mixing) several layers contribute to the LEIS signal after a few minutes. After about half an hour of bombardment, the Pd contribution to the LEIS signal for both samples reaches values below the nominal ones. This is due, as described above, to preferential sputtering of Pd by

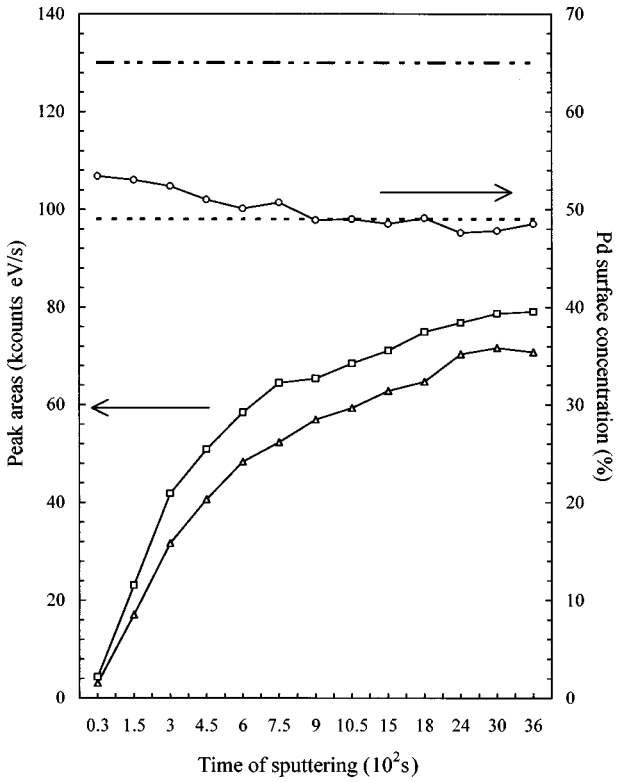

FIG. 7. LEIS study of a thin slice of the $Pd_{65}Pt_{35}$ rod. The sample has been previously bombarded with 1-keV He ions until it reaches its equilibrium composition (dotted line) under sputtering and then exposed to residual atmosphere (see text). The dashed-dotted line represents the nominal composition. The squares, triangles, and circles represent, respectively, the absolute Pd and Pt intensities as a function of sputtering time and the corresponding Pd concentration.

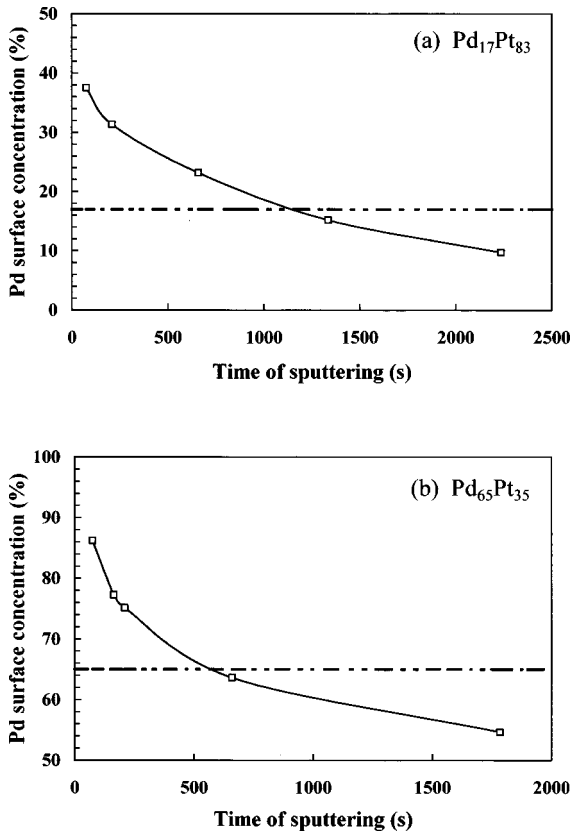

FIG. 8. Evolution of Pd surface concentration as deduced from the quantification of the Pd and Pt peaks areas (see Figs. 5 and 6). (a) $Pd_{17}Pt_{83}$ and (b) $Pd_{65}Pt_{35}$. The dashed-dotted lines represent the nominal compositions.

the ion beam. Indeed, it is well known that the sputtering of an element is related to its cohesive energy and, actually, the sputtering yield increases when the cohesive energy decreases.[26]

IV. MODELING OF THE SEGREGATION

A. Formulation of the model

In order to better understand previous experimental results concerning the surface segregation in bulk alloys,[6,7] we have developed an energetical model.[17–19] This model uses the concept of equivalent medium approximation, which allows us to calculate concentration-dependent pair interactions. Bond-strength modifications at surfaces are taken into account through an empirically modified tight-binding approach in the second moment approximation. This model includes elastic strain effects for alloys of elements with different sizes and has already been applied to fcc monocrystalline Pd-*X* alloys including the PdPt bimetallic system. The PdPt system is a nearly regular exothermic alloy with low heat of mixing[27] and for which no strong size effects are expected since the atomic radii of the two components are rather similar (1% mismatch). The main results are a strong Pd segregation for both (111) and (100) orientations, but smaller for the closest-packed surface, and the depth profile behavior is very simple, as expected. Damped oscillations in concentration are observed in the whole composition range and the bulk composition is nearly reached for the third atomic layer. This is consistent with a low negative heat of mixing. Indeed, unlike atoms prefer to be adjacent in an exothermic alloy.

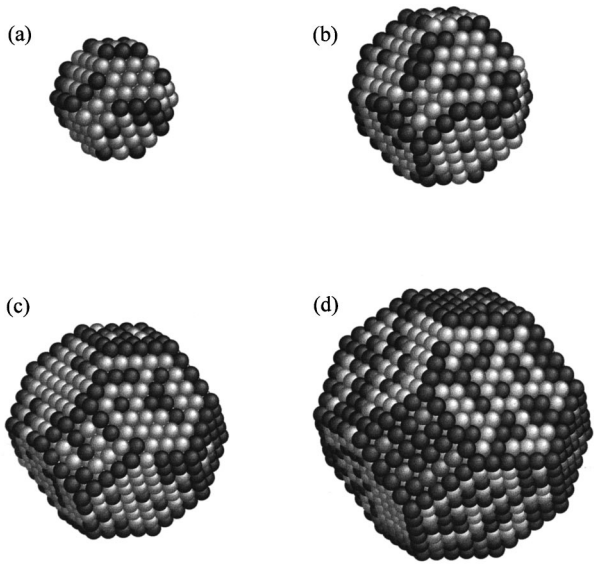

FIG. 9. Results of Monte Carlo simulations of $Pd_{17}Pt_{83}$ bimetallic clusters. (a) 201-, (b) 586-, (c) 1289-, and (d) 2406-atom cubo-octahedron clusters. Black and gray spheres represent, respectively, Pd and Pt atoms.

TABLE I. Segregation statistics for $Pd_{17}Pt_{83}$ clusters.

$Pd_{17}Pt_{83}$ system. Particle size (nm)	Particle size (number of atoms)	Fractional surface coverage by Pd atoms (%)	Fractional corner and edge coverage by Pd atoms (%)	Number of surface Pd neighbors per Pd surface atom	Fraction of Pd in the interior of the particles (%)
1.8	201	27.4	45.0	1.06	0.0
2.6	586	36.1	71.9	2.02	0.6
3.4	1289	44.0	86.4	2.38	0.7
4.2	2406	52.1	92.3	2.8	0.9

For semi-infinite systems, the bulk provides an unlimited supply of atoms, whereas for small particles, the number of atoms and thus the supply is finite. In such a case, the calculations must use a Monte Carlo technique to take into account the constraint of the mass balance. In our Monte Carlo simulations, the input data of the model are the pair-interaction energies of atoms in different binding sites, i.e., sites energies, in clusters of truncated cubo-octahedral shape, since it has been shown[18] that this is the stable shape. The Monte Carlo technique has previously been used to study the surface segregation in bimetallic systems.[19,28,29] Basically, for an A-B alloy one starts with the desired number of A and B atoms randomly distributed on the lattice sites of the particle. The initial configuration energy is calculated from the pair bond energies. Later on, A and B atoms are allowed to exchange their positions if the resulting change in the configuration energy ΔE is negative. The atoms can also switch their positions if the energy change is positive but, in this case, $e^{(-\Delta E)/(kT)}$ must be greater than a random number lying between 0 and 1. This cycle is repeated for all of the atoms several hundred times until the configurational energy is stabilized.

B. Results and discussion

In the present work, we apply the MC-MTB interaction potential to the $Pd_{17}Pt_{83}$ and $Pd_{65}Pt_{35}$ truncated cubo-octahedral clusters. In the laser source, the nucleation energy (brought by each atom during the nucleation process) is sufficient to allow reorganization of the system before quenching due to collisions with helium atoms. Since the melting temperature for small clusters is known to be much lower than the bulk one[30] a temperature of 600 K has been taken for the simulations. The total number of atoms in the clusters varies from 201 to 2406, representing particle diameters ranging from about 1.8 up to 4.2 nm. This roughly corresponds to the real sizes of the systems as deduced from electron microscopy experiments. At this stage, we need to mention that the morphology of the clusters would not affect significantly the segregation process. Indeed, if we compare, for each studied size or dispersion, the mean surface coordination numbers (which, in fact, govern mainly the surface composition) of cubo-octahedrons [with triangular (100) faces] and truncated octahedrons [with square (100) faces] we notice that they do not differ by more than 0.6.

A typical MC simulation result for the $Pd_{17}Pt_{83}$ system is shown in Fig. 9. The following important features are noticed: Pd segregates to the surface for all cluster sizes but the surface Pd concentration clearly increases as the size increases. For small sizes [Fig. 9(a)] the mass balance effect coupled with the low Pd content plays an important role and *only the low-coordinated sites* (i.e., corners and edges) are occupied by the segregating element. For larger sizes [Figs. 9(c) and 9(d)], the proportion of surface atoms decreases and hence the supply of Pd atoms is now sufficient to fill more coordinated planar faces (100) and (111). When going from 201 atoms to 2406 atoms clusters, the surface concentration increases from 27.4% to 52.1% as stated in Table I. To compare experimental results and simulations we assume, in a very simple way, that the LEIS signal of a cluster is proportional to its projected surface on the flat support. Taking into account the size histogram of $Pd_{17}Pt_{83}$ and weighting each class of size (i.e., of projected surface) by the predicted Pd concentration, one calculates a mean Pd surface concentration of 37%.

Concerning the $Pd_{65}Pt_{35}$ alloy, the arguments developed above hold, but in this case, the mass balance effect is much less pronounced. For example the 201 atoms cluster has 122 surface sites and 130 Pd atoms: so one has the possibility of

TABLE II. Segregation statistics for $Pd_{65}Pt_{35}$ clusters.

$Pd_{65}Pt_{35}$ system. Particle size (nm)	Particle size (number of atoms)	Fractional surface coverage by Pd atoms (%)	Fractional corner and edge coverage by Pd atoms (%)	Number of surface Pd neighbors per Pd surface atom	Pd fraction in the interior of the particles (%)
1.8	201	93.1	98.3	5.08	20.3
2.6	586	95.5	99.0	5.22	39.2
3.4	1289	97.2	100	5.43	45.5
4.2	2406	98.6	100	5.52	49.6

covering the entire surface with Pd. Actually, the Pd surface concentration rises up to 93.1% for this small cluster and up to 98.6% for the 2406 atoms cluster. All the calculated results corresponding to this alloy are presented in Table II. The main result that has to be noted is that the surface is almost entirely covered by Pd atoms whatever the size of the cluster. By applying to the $Pd_{65}Pt_{35}$ histogram the weighting procedure described above, one obtains a mean Pd surface concentration of 96%. Finally, a strong Pd segregation is evidenced for both alloys and in the whole range of cluster sizes. The mass balance effect is shown to play an important role for small clusters especially for a low content of the segregating element.

V. CONCLUSION

Model supported Pd-Pt clusters have been produced by low-energy cluster beam deposition. TEM-EDX analysis reveals a narrow size range and a small dispersion of the particle composition for both $Pd_{65}Pt_{35}$ and $Pd_{17}Pt_{83}$ alloys. The use of the laser source appears to be a unique way of preparing model bimetallic clusters of uniform size and composition. The surfaces of the clusters are strongly enriched in Pd as determined by LEIS, which has been shown to give reliable results for dispersed materials. This result is in agreement with Monte Carlo simulations based on an adjusted tight-binding potential, which additionally predict that Pd segregation in small Pd-Pt particles takes place especially at low-coordinated sites. This detailed description of the catalytic sites at the atomic scale will certainly be of great help in the interpretation of the catalytic behavior of PdPt bimetallic aggregates.

ACKNOWLEDGMENTS

The authors thank G. Guiraud and C. Clavier for technical assistance and P. Delichère for providing them with the LEIS results on the monocrystalline Pt sample. We also thank C. Leclercq for the EDX measurements and Dr. N. S. Prakash for a critical reading of the manuscript.

*Author to whom correspondence should be addressed.

[1] J. H. Sinfelt, J. Catal. **29**, 308 (1973).
[2] J. H. Sinfelt, G. H. Via, and F. W. Lytle, J. Chem. Phys. **72**, 4832 (1980).
[3] S. A. Stanislaus and B. H. Cooper, Catal. Rev. Sci. Eng. **36**, 75 (1994).
[4] H. H. Brongersma, M. J. Sparnaay, and T. M. Buck, Surf. Sci. **71**, 657 (1978).
[5] P. Varga and G. Hetzendorf, Surf. Sci. **162**, 544 (1985).
[6] P. Miegge, J. L. Rousset, B. Tardy, J. Massardier, and J. C. Bertolini, J. Catal. **149**, 404 (1994).
[7] J. C. Bertolini, J. L. Rousset, P. Miegge, J. Massardier, B. Tardy, Y. Samson, B. C. Khanra, and C. Creemers, Surf. Sci. **281**, 102 (1993).
[8] *Surface Segregation Phenomena*, edited by P. A. Dowben and A. Miller (CRC Press, Boca Raton, FL, 1990).
[9] W. K. den Otter, H. H. Brongersma, and H. Feil, Surf. Sci. **306**, 215 (1994).
[10] H. Miura, S. Feng, R. Saymeh, and R. D. Gonzalez, in *Catalysis Characterization Science*, edited by M. L. Deviney and J. L. Gland, ACS Symposium Series No. 288 (American Chemical Society, Washington, DC, 1985), p. 294.
[11] O. B. Yang and S. I. Woo, in *Proceedings of the 10th International Congress on Catalysis*, Budapest, 1992, edited by L. Guczi, F. Solymosi, and P. Tetenyi (Elsevier, New York, 1993), Vol. A, p. 671.
[12] M. J. Lopes, P. A. Macros, and J. A. Alone, J. Chem. Phys. **104**, 1056 (1996).
[13] S. Valkealahti and M. Manninen, Phys. Rev. B **45**, 9459 (1991).
[14] C. L. Cleveland and U. Landman, J. Chem. Phys. **94**, 7376 (1991).
[15] J. M. Montejano-Carrizales, M. P. Iniguez, and J. A. Alonso, Phys. Rev. B **49**, 16 649 (1994).
[16] L. Yang and A. E. DePristo, J. Catal. **148**, 575 (1994).
[17] J. L. Rousset, J. C. Bertolini, and P. Miegge, Phys. Rev. B **53**, 4947 (1996).
[18] J. L. Rousset, A. M. Cadrot, F. Santos Aires, A. Renouprez, P. Melinon, A. Perez, M. Pellarin, J. L. Vialle, and M. Broyer, J. Chem. Phys. **102**, 8574 (1995).
[19] J. L. Rousset, B. C. Khanra, A. M. Cadrot, F. J. Cadete Santos Aires, A. Renouprez, and M. Pellarin, Surf. Sci. **352-354**, 583 (1996).
[20] P. Milani and W. A. de Heer, Rev. Sci. Instrum. **61**, 1835 (1990).
[21] G. Fuchs, P. Mélinon, F. Santos Aires, M. Treilleux, B. Cabaud, and A. Hoareau, Phys. Rev. B **44**, 3926 (1991).
[22] B. Tardy, C. Noupa, C. Leclerc, J. C. Bertolini, A. Hoareau, M. Treilleux, J. P. Faure, and G. Nihoul, J. Catal. **129**, 1 (1991).
[23] J. C. Bertolini, J. L. Rousset, P. Miegge, J. Massardier, and B. Tardy, Surf. Sci. **287/288**, 346 (1993).
[24] S. H. Overbury, R. J. A. van den Oetelaar, and D. M. Zehner, Phys. Rev. B **48**, 1718 (1993).
[25] L. C. A. van den Oetelaar, O. W. Nooij, S. Oerlemans, A. W. Denier van der Gon, H. H. Brongersma, L. Lefferts, A. G. Roosenbrand, and J. A. R. van Veen, J. Phys. Chem. B **102**, 3445 (1998).
[26] *Practical Surface Analysis*, edited by D. Briggs and M. P. Seah, Ion and Neutral Spectroscopy, 2nd ed. (Wiley, Chichester, 1992), Vol. 2.
[27] J. B. Darby and K. M. Myles, Metall. Trans. A **3**, 653 (1992).
[28] R. G. Donnely and T. S. King, Surf. Sci. **74**, 89 (1978).
[29] J. K. Strohl and T. S. King, J. Catal. **116**, 540 (1989).
[30] C. Rey, L. J. Gallego, J. Garcia-Rodeja, J. A. Alonso, and M. P. Iniguez, Phys. Rev. B **48**, 8253 (1993).